Electronic Supplementary Material (ESI) for Physical Chemistry Chemical Physics.

Supplementary Information

Self-assembly polymorphism of 2,7-bis-nonyloxy-9-fluorenone: solvent induced the diversity of intermolecular dipole–dipole interaction

Lihua Cui, Xinrui Miao, Li Xu, Yi Hu and Wenli Deng**

College of Materials Science and Engineering, South China University of Technology, Guangzhou 510640, P.R. China

E-mail Address: msxrmiao@scut.edu.cn; wldeng@scut.edu.cn

Corresponding author: College of Materials Science and Engineering,
South China University of Technology,
Wushan Road, Tianhe District, Guangzhou 510640, P. R. China.
Tel: (+86) 020-22236708
E-mail: msxrmiao@scut.edu.cn; wldeng@scut.edu.cn

Table S1. Chemical structures of 2,7-bis-nonyloxy-9-fluorenone (F−OC_9) and solvents

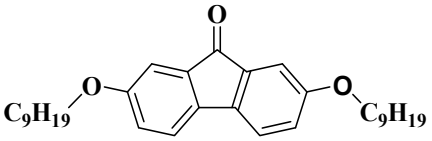

solvent	1-phenylotane	n-tetradecane	1-octanol	dichloromethane	alkylated acids
	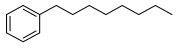		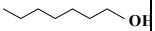	CH_2Cl_2	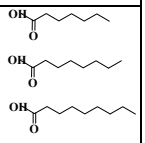

Fig. S1 Semiempirically calculated charge density contours of the HOMO for F–OC_9.

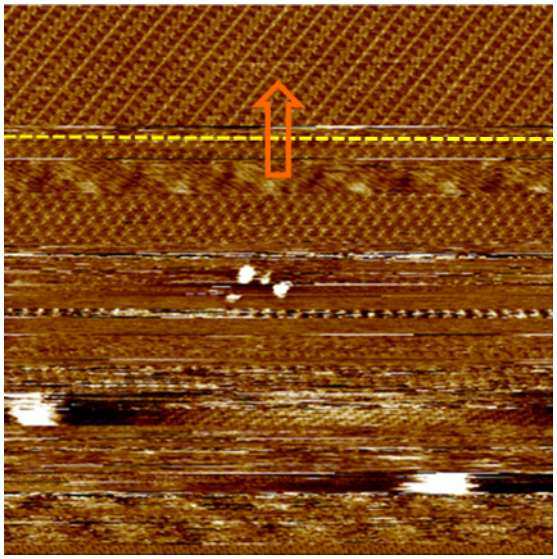

Fig. S2 STM shows the phase transition of F–OC_9 from a butterfly pattern to alternating pattern. Orange arrow indicates the direction of the scanning and the dotted yellow line indicates the position at which the structure changed. Notably, the transformation occurred almost instantaneously. (Scan area: 120 × 120 nm^2. V_{bias} = 650 mV, I_t = 580 pA)

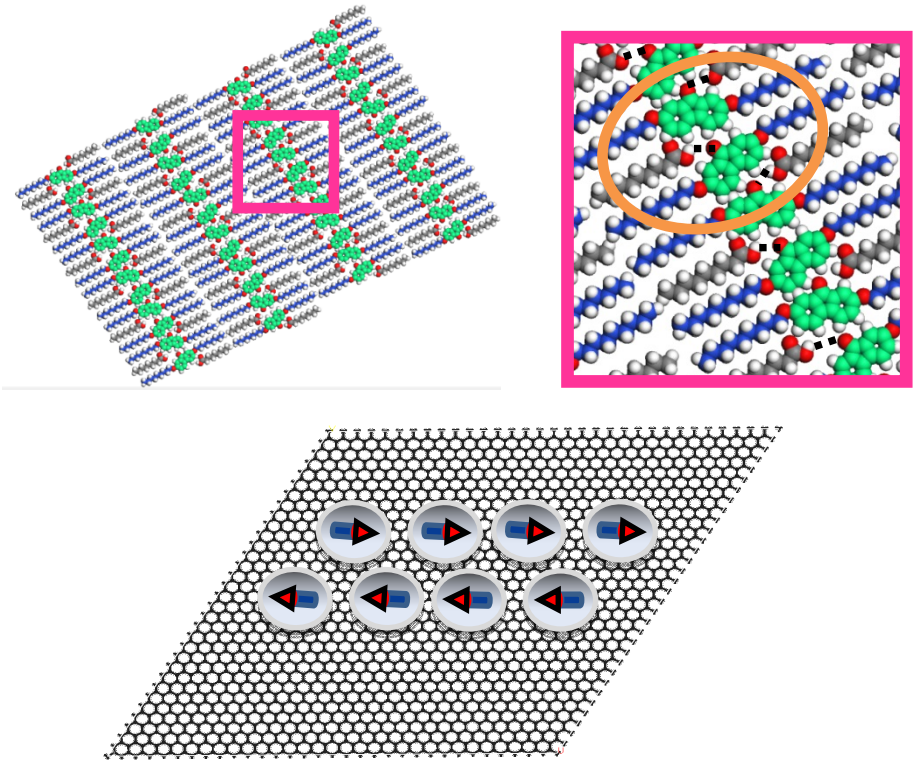

Fig. S3 The details of arrangement of linear coadsorption phase of F–OC_9 at heptanoic acid/HOPG interface. The sequential head-to-tail arrangement of fluorenone cores separates neighboring molecular dipole pairs to enhance dipole interactions thus lower the electronic potential.

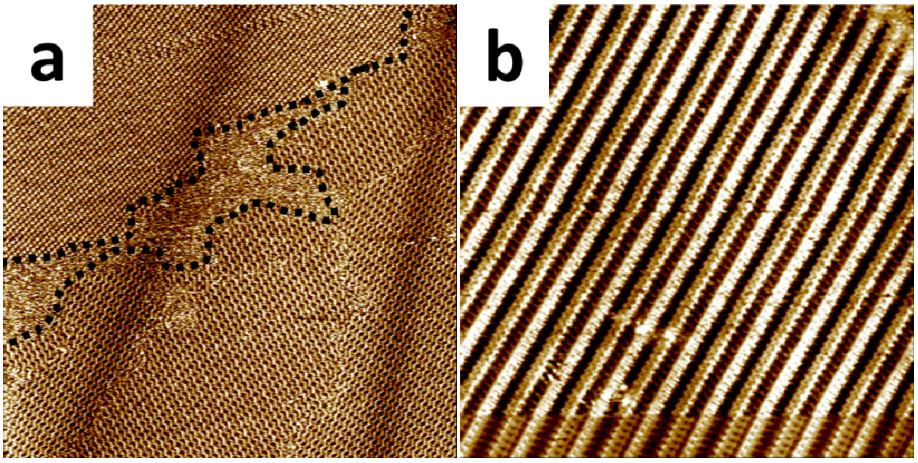

Fig. S4 (a) Large-scale STM image of F–OC_9 self-assembly in octanoic acid on HOPG surface showing the coexistence of "lips" and semi-circle like structures at medium concentration. (Scan area: 200 × 200 nm^2. V_{bias} = 640 mV, I_t = 520 pA) (b) Coadsorbed linear phase of F–OC_9 self-assembly in octanoic acid showing the whole area is covered by linear arranged F–OC_9 and solvent molecules at a low concentration. (Scan area: 65 × 65 nm^2. V_{bias} = 630 mV, I_t = 520 pA)

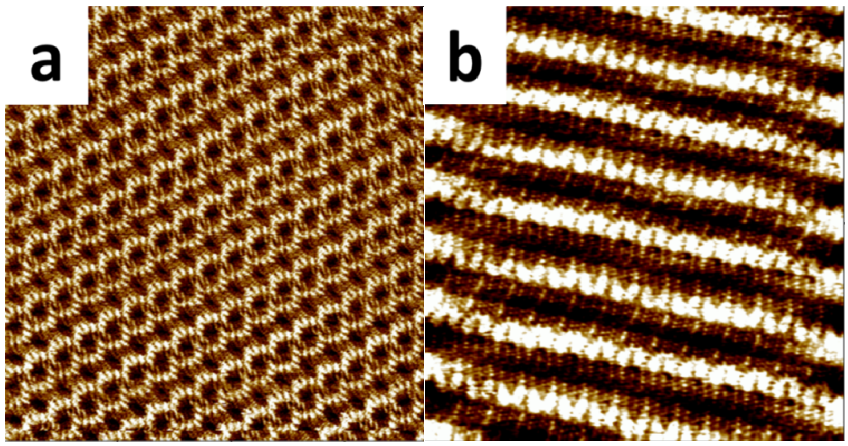

Fig. S5 High-resolution STM image of F–OC_9 self-assembled adlayer in nonanoic acid on HOPG surface. (a) Semi-circle like pattern. (Scan area: 37 × 37 nm^2. V_{bias} = 630 mV, I_t = 505 pA) (b) Linear coadsorbed pattern. (Scan area: 20 × 20 nm^2. V_{bias} = 630 mV, I_t = 505 pA)

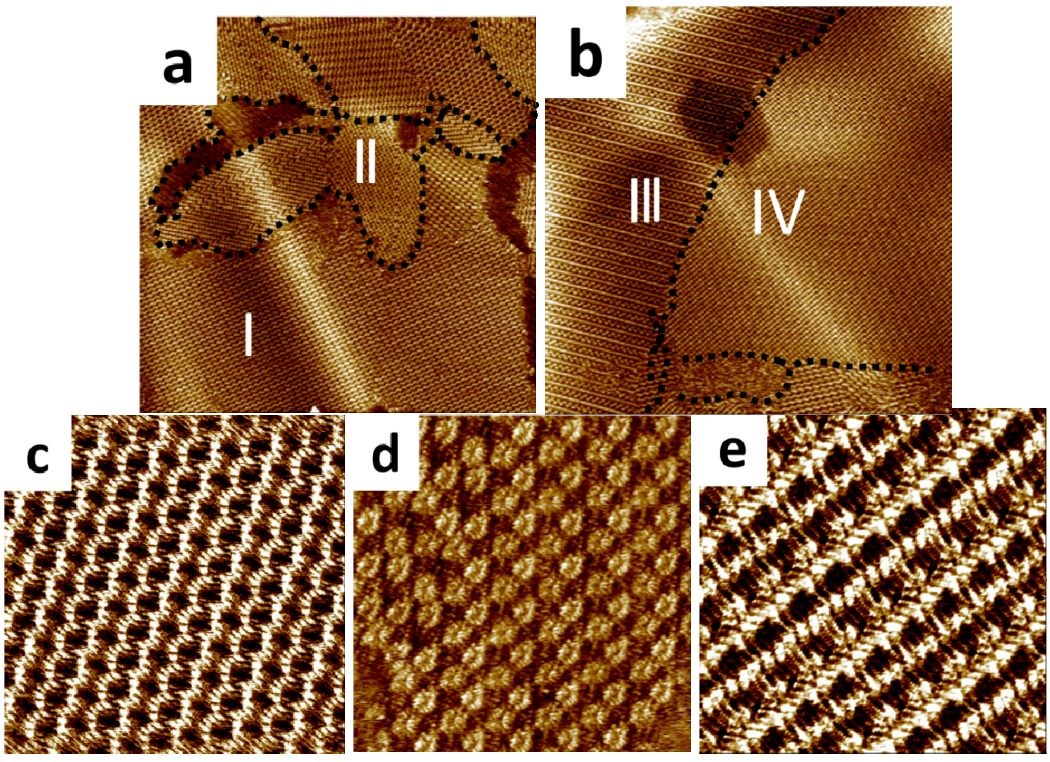

Fig. S6 (a, b) Typical STM images of F–OC_9 self-assembly in 1-phenyloctane showing the coexistence of three different assembled patterns. (Scan area: 200 × 200 nm^2. V_{bias} = 650 mV, I_t = 580 pA). (c, d and e) High-resolution STM images of F–OC_9 in 1-phenyloctane showing (c) the semi-circle like pattern (37 × 37 nm^2), (d) the "lips" like pattern (18 × 18 nm^2) and (e) the alternating structure (10 × 10 nm^2).

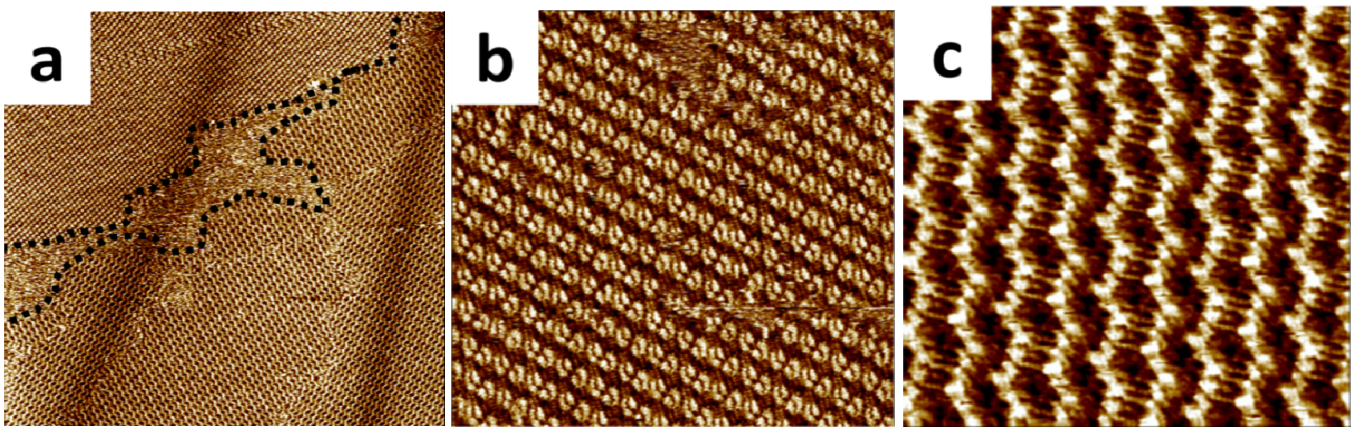

Fig. S7 (a) Typical STM images of F–OC_9 self-assembly in *n*-tetradecane showing the coexistence of assembled patterns. (Scan area: 200 × 200 nm^2. V_{bias} = 650 mV, I_t = 580 pA). (b, c) High-resolution STM images of F–OC_9 in *n*-tetradecane showing (b) the "lips" like pattern (39 × 39 nm^2) and (c) the semi-circle like pattern (20 × 20 nm^2).

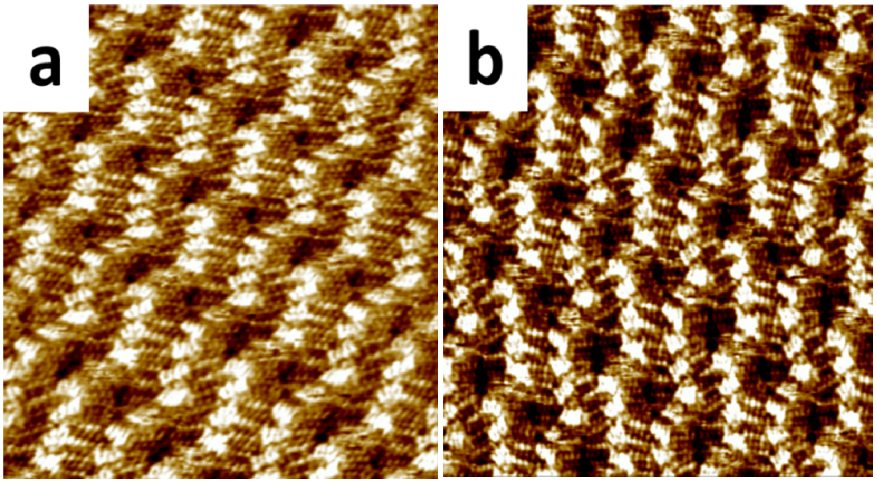

Fig. S8 High-resolution STM images of F–OC_9 self-assembled in (a) 1-octanol (Scan area: 200 × 200 nm^2. V_{bias} = 788 mV, I_t = 463 pA) and (b) dichloromethane on the HOPG surface after the samples were placed more than two hours (Scan area: 200 × 200 nm^2. V_{bias} = 795 mV, I_t = 457 pA).

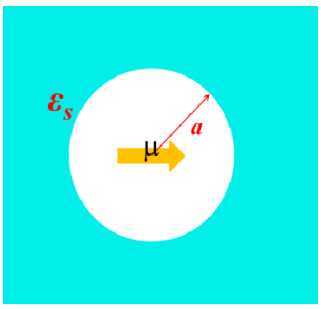

Fig. S9 Spherical cavities point dipole model of Onsager. Diagram of Onsager reaction field model: solute molecules are seated in a radius of a circular hole, which is surrounded by a continuous medium with the dielectric constant ε_s. (μ is dipole moment)

solvation energy:

$$\Delta F_{el} = \frac{1}{a^3}\frac{(\varepsilon_s - 1)}{(2\varepsilon_s + 1)}\mu^2$$

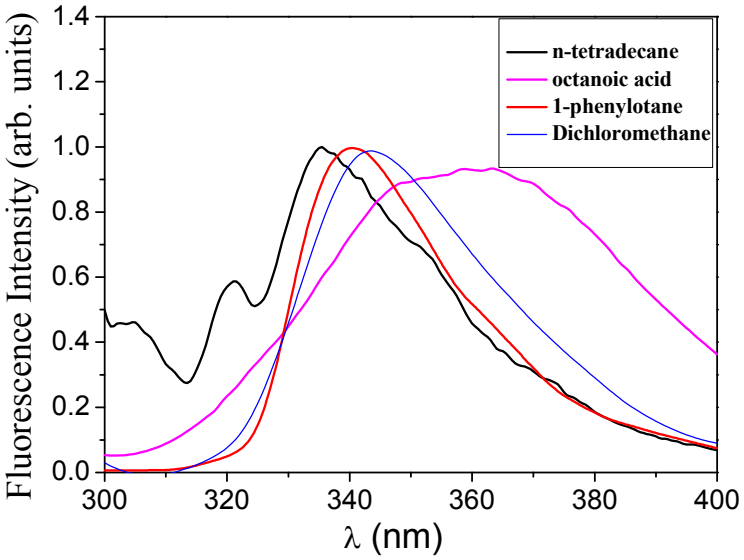

Fig. S10 Normalized emission spectra of F–OC_9 measured in *n*-tetradecane, octanoic acid, 1-phenylotane and dichloromethane (λ_{ex} = 228 nm).

The fluorescence emitted was observed perpendicularly to the direction of the exciting beam. Samples for fluorescence measurements were prepared using a 0.2 cm high sensitivity micro quartz cell. The concentration of the solutions studied was ca. 10^{-6} mol L^{-1}. The luminescence spectra reported have been corrected for the spectral response of the photomultiplier (Hamamatsu R-928) and monochromator pass, but not for reabsorption which was negligible in these samples.

Figure S10 shows a typical example of the solvent effect on the electronic emission spectrum of F–OC_9. The fluorescence intensity distribution is described by a Gaussian shape. The observed spectral shifts are correlated with the polarity parameters (dielectric constant and refractive index) of solvents. It is inferred

from the plot that changes in the dipole moment and nature of the solvent can cause wavelength shifts to the excited state of substituted fluorenones.

S.11

The general form of the dipole–dipole interaction can be found in many text books and is of the form: For Two dipoles, dipole moments u1 and u2, with polar orientations θ1 and θ2. Φ is the azimuthal orientation of u2 in reference to u1. See figure. (far field approximation) (Intermolecular and Surface Forces, J. N. Israelachvili 3rd ed., p81)

$$U(r,\theta 1,\theta 2,\Phi) = -\frac{u1.u2}{4\pi\epsilon\epsilon_0 r^3}[2\cos(\theta_1)\cos(\theta_2) - \sin(\theta_1)\sin(\theta_2)\cos(\varphi)] \quad (1)$$

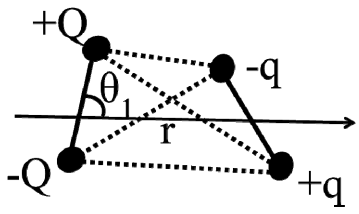

If we consider two key cases: A) head to tail orientation and (B) head – to-head orientation.

A) Head-to-tail arrangement →→

$\theta_1=\theta_2=0$, $\sin(\theta_1) = 0 = \sin(\theta_2)$, $\cos(\theta_1) = 1 = \cos(\theta_2)$

$$U(r,\theta 1,\theta 2,\Phi) = -\frac{u1.u2}{4\pi\epsilon\epsilon_0 r^3}[2\cos(\theta_1)\cos(\theta_2) - \sin(\theta_1)\sin(\theta_2)\cos(\varphi)]$$

Becomes: $U(r,\theta 1,\theta 2,\Phi) = -\frac{2u1.u2}{4\pi\epsilon\epsilon_0 r^3}$ (2)

Negative indicating a low energy, stable arrangement.

B) Head-to-tail arrangement →←

$\theta_1=0$, $\theta_2=180°$, $\sin(\theta_1) = 0 = \sin(\theta_2)$, $\cos(\theta_1) = 1$, $\cos(\theta_2) = -1$

$$U(r,\theta 1,\theta 2,\Phi) = -\frac{u1.u2}{4\pi\epsilon\epsilon_0 r^3}[2 * 1 * -1]$$

$$U(r,\theta 1,\theta 2,\Phi) = +\frac{2u1.u2}{4\pi\epsilon\epsilon_0 r^3} \quad (3)$$

POSITIVE: high energy, unstable geometry.

Similar calculations also can be used to show that ↑↓ is also stable, i.e. collinearly arranged and antiparallel arranged dipole are most stable interaction.

Moreover, Equation (1) also shows that for two equal dipoles of moments 1 D, their interaction energy in a vacuum will equal kT at r ~ 0.36 nm (T=300K) when the dipoles are in line and at r ~ 0.29 nm when parallel (or antiparallel). Since these distances are of the order of molecular separations in solids and liquids, we see that at normal temperatures dipolar interactions (alone) are strong enough to bind only very polar molecules. Thus, $U(r, \theta 1, \theta 2, \Phi)$/mol = 2.49118kJ/mol. Here, according to this estimation, we evaluate the dipole interaction for "lips" shaped and alternating pattern.

S.12

Methods used for estimating enthalpy and entropy values are often forced to simplify molecular systems, a common example being simulations that **ignore the presence of substrate or solvent** to reduce computation time.

In order to estimate the chain-chain van der Waals interaction energies, we computed dimers of nonane at different distances and found a value of 20.14 kJ mol^{-1} at the equilibrium distance of 4.5 Å. It corresponds to approximately 4.5 kJ mol^{-1} per C_2 unit, and for the chain lengths used in our experiments, we thus obtain an average interaction energy of 40.5 kJ mol^{-1} (C18). This value is in the range of an average dimer bonding energy. Thus, when discussing possible structures one has to make sure that neighboring chains can interact in the best possible way. The average values of the chain – chain distances in the STM pictures (approximately 4.5 Å for alternating phase and 4.1 Å for "lips" shaped phase) fit well with the equilibrium distance found in the computations. For a more quantitative analysis, we fitted the data of the the nonane dimers to a morse potential $V(r) = D[1 - \exp(-\alpha(r - r_0)^2)]$, where D = 20.14 kJ mol^{-1}, α = 5.0 $Å^{-2}$, and r_0 = 4.5 Å. Thus according to the given distance, we can use this potential to estimate the intermolecular alkyl chain interactions for alternating and "lips" shaped patterns. The values of the chain – chain van der Waals interaction are 40.5 kJ Mol^{-1} for alternating phase and 35.143 kJ Mol^{-1} for "lips" shaped structure respectively.

Table S2. Schematic representation and unit cell parameters of all phases observed in 2D self-assembly monolayers of F–OC_9 dissolved in seven solvents on HOPG surface under different concentrations

Solvent	Structure model	Concentration (mol L^{-1})	a (nm)	b (nm)	α (°)	Molecules per unit	S (nm^2 per molecule)	Density
heptanioc acid	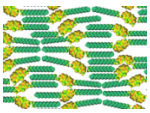	>10-4 ~saturated	2.4 ± 0.2	2.3 ± 0.1	93 ± 1	5	0.55	1.81
	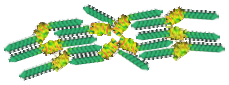	~10^{-5}	5.4 ± 0.1	2.7 ± 0.2	77.89	7	0.90	1.12
	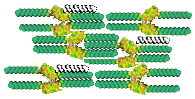		2.8 ± 0.2	2.6 ± 0.1	111 ± 1	4	1.08	0.92
	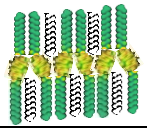	<10^{-6}	1.5 ± 0.1	2.6 ± 0.2	89 ± 2	2	1.02	0.98
octanoic acid	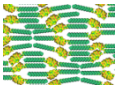	~10^{-5}	2.6 ± 0.2	2.2 ± 0.2	90 ± 1	5	0.56	1.78
	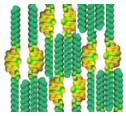	~10^{-5}	1.7 ± 0.1	1.6 ± 0.1	126 ± 1	2	0.89	1.12
	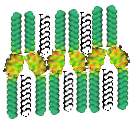	<10^{-6}	1.6 ± 0.2	2.5 ± 0.1	99 ± 1	2	1.10	0.91
Nonanoic acid	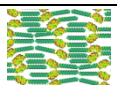	>10^{-4} ~saturated	2.6 ± 0.1	2.3 ± 0.1	87 ± 2	5	0.56	1.79
	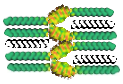	~10^{-5}	2.9 ± 0.2	1.5 ± 0.1	100 ± 2	2	1.18	0.84
	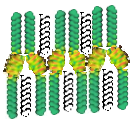	<10^{-6}	1.6 ± 0.2	3.1 ± 0.1	99 ± 1	2	1.28	0.78
1-phenylotane	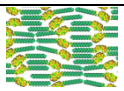	___	2.4 ± 0.1	2.3 ± 0.1	94 ± 2	5	0.55	1.81
	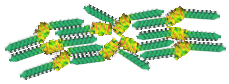	___	5.4 ± 0.1	2.5 ± 0.2	79.56	7	0.82	1.21
	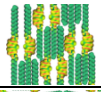	___	1.8 ± 0.2	1.6 ± 0.2	125.07	2	0.89	1.11
n-tetradecane	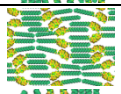	___	2.5 ± 0.1	2.2 ± 0.1	92 ± 2	5	0.54	1.85
		___	1.8 ± 0.2	1.6 ± 0.1	124.13	2	0.90	1.10
	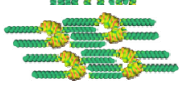	<10^{-5}	2.0 ± 0.2	2.1 ± 0.1	119 ± 1	2	1.38	0.73
dichloromethane methanol ethanol	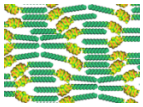	___	2.4 ± 0.1	2.2 ± 0.1	92 ± 1	5	0.52	1.90